A Comparative Olfactory MRI, DTI and fMRI Study of COVID-19 Related Anosmia and Post Viral Olfactory Dysfunction

Duzgun Yildirim, MD, Sedat Giray Kandemirli, MD, Deniz Esin Tekcan Sanli, MD, Ozlem Akinci, MD, Aytug Altundag, MD

Rationale and Objective: To evaluate how COVID-19 anosmia imaging findings resembled and differed from postinfectious olfactory dysfunction (OD).

Material and Methods: A total of 31 patients presenting with persistent COVID-19 related OD and 97 patients with post-infectious OD were included. Olfactory bulb MRI, DTI and olfactory fMRI findings in both groups were retrospectively assessed.

Results: All COVID-19 related OD cases were anosmic, 18.6% of post-infectious OD patients were hyposmic and remaining 81.4% were anosmic. Mean interval between onset of OD and imaging was 1.5 months for COVID-19 related OD and 6 months for post-infectious OD. Olfactory bulb volumes were significantly higher in COVID-19 related OD than post-infectious OD. Deformed bulb morphology and increased olfactory bulb signal intensity was seen in 58.1% and 51.6% with COVID-19 related OD; and 63.9% − 46.4% with post-infectious OD; without significant difference. Significantly higher rate of olfactory nerve clumping and higher QA values at orbitofrontal and entorhinal regions were observed in COVID-19 related OD than post-infectious OD.
Absence of orbitofrontal and entorhinal activity showed no statistically significant difference between COVID-19 related OD and post-infectious OD, however trigeminosensory activity was more robust in COVID-19 related OD cases.

Conclusion: Olfactory bulb damage may play a central role in persistent COVID-19 related anosmia. Though there is decreased olfactory bulb volume and decreased white matter tract integrity of olfactory regions in COVID-19 related anosmia, this is not as pronounced as in other post-infectious OD. Trigeminosensory activity was more robust in COVID-19 related OD. These findings may reflect better preserved central olfactory system in COVID-19 related OD compared to COVID-19 related OD.

Key Words: olfactory bulb MRI; COVID; infection; anosmia; smell.

INTRODUCTION

Olfactory dysfunction (OD) gained widespread attention among the public and medical community as post COVID-19 hyposmia and anosmia cases have surged since the start of the pandemic (1). OD in COVID-19 has been reported up to 80% in some series, and may be seen as an isolated symptom, precede the respiratory manifestations or develop after onset of respiratory symptoms (2,3). Majority of the patients with COVID-19 OD recover spontaneously within two weeks; however persistent severe OD may persist in 7%–8% 2 months after onset (4-6). OD can also be post-infectious due to other viral pathogens, post-traumatic, secondary to sinonasal disease or part of neurodegenerative disease processes (7,8). Upper respiratory tract infections account as 1 of the most common identifiable cause of OD, with post-infectious cases constituting 22%-36% of all olfactory loss cases (9,10). The pathogenesis of COVID-19 anosmia is still debated, however evidence suggests features distinct from the obstructive etiology of the OD in other viral upper respiratory tract infections, as there is a lower prevalence of sinonasal symptoms in COVID-19 related OD (1,11). Proposed mechanisms for COVID-19 anosmia are olfactory recess obstruction/inflammation and/or olfactory bulb damage (12).

OD may occur due to disruption of the olfactory system at different pathways, which can be evaluated with different imaging modalities. Paranasal sinus CT allows assessment for obstructive causes, whereas magnetic resonance imaging (MRI) provides morphological data about olfactory nerve, bulb and primary/secondary olfactory cortices (13,14). Diffusion tensor imaging (DTI) can also be used to assess olfactory network and microstructural properties of the white matter (15-18). Odor-stimulated functional MRI has also been used in assessment of OD in neurodegenerative disease and post-traumatic anosmia (19,20).

Despite the high prevalence of COVID-19 related OD, there is limited data on MR imaging findings, which might be related to generally transient nature of the symptoms, re-allocation of health resources during the pandemic and reluctance of the patients to seek medical care for OD. Limited imaging data derived from case reports or case series have reported conflicting findings. (1,21-24). Part of this discrepancy might be related to patient selection criteria and variations in imaging protocols. Our group had previously reported olfactory bulb MRI findings in 23 cases with persistent COVID-19 anosmia, and reported a high percentage of abnormal olfactory bulb signal intensity and contour changes (25).

An imaging study that includes a comparison group and incorporates advanced techniques like DTI and olfactory fMRI could be helpful to better understand the underlying pathogenesis, and guide patient management for cases with persistent OD. As a follow-up study, we assessed the olfactory bulb MRI, DTI and olfactory fMRI findings in persistent COVID-19 anosmia; and compared the findings to post-infectious olfactory loss related to other pathogens.

MATERIALS AND METHODS

Study Population

COVID-19 related OD group included patients presenting with olfactory dysfunction after COVID-19 infection to our Smell and Taste Center Clinic between May 2020 and March 2021. Inclusion criteria were: (1) sudden loss of smell, (2) COVID-19 infection confirmed during initial symptoms by polymerase chain reaction (PCR) with a swab test, (3) persistence of OD for minimum 1-month without any treatment/intervention for OD. There was a total of 31 patients presenting with persistent COVID-19 related OD with a mean age of 32.5±10.8 years that completed subsequent olfactory assessment and imaging tests.

Post-infectious OD group consisted of patients presenting with olfactory dysfunction after upper respiratory tract infection to our center between May 2016-March 2020. There was a total of 97 patients with post-infectious OD with a mean age of 45.9±13.5 years that completed subsequent olfactory assessment and imaging tests.

Exclusion criteria for both groups were cases with preexisting smell and taste dysfunction, prior head trauma and history or evidence of allergic rhinitis and chronic rhinosinusitis.

This study has been approved by the local institutional review board and informed consent prior to participation in the study was provided by all patients.

Olfactory Assessment

After a detailed anamnesis including onset/course of the olfactory dysfunction and accompanying sinonasal symptoms like nasal congestion and rhinorrhea; otolaryngological examination was performed. Olfactory dysfunction was evaluated objectively with Sniffin' Stick Test (Burghart Messtechnik, Wedel, Germany) which is performed with odor-containing felt-tip pens (26). This test assesses bilateral odor detection thresholds (T), odor discrimination (D), and odor identification (I) with a scale of 1−16 for each component. TDI is the summative score of the three components; and olfactory function is categorized as normosmia: scores $\geq$ 30.5, hyposmia: scores between 16.5 and 30.5, and anosmia: scores <16.5 (27).

MRI Protocol

Olfactory bulb MRI was acquired with a 3T scanner (Magnetom, Siemens, Erlangen, Germany) with a 32-channel head coil. In addition to conventional sequences for whole brain, sequences dedicated to the olfactory system included high resolution T2-SPACE sagittal images, coronal T2 images with a field of view (FOV) covering anterior pole of the olfactory bulb to the primary olfactory region, as described previously (14,25).

Diffusion tensor images were acquired in the axial plane extending from craniocervical junction to vertex using a single-shot, diffusion-weighted EPI sequence with a b value of 1000 seconds/mm^2 in 64 diffusion encoding directions (Supplement 1). n-butanol (4% v/v) was the preferred olfactory stimuli during olfactory fMRI. n-butanol stimulates both olfactory and trigeminal nerve with a bimodal percept (28,29). fMRI images were obtained in a 4-minute 2-block design consisting of 1) continuous odor exposure for 2 minutes and 2) normal breathing blocks with continuous flow of odorless air with 50% relative humidity at room temperature for 2 minutes. Odors were presented to participants via nasal cannula with continuous air flow at a rate of 4 L/min (Supplement 1). Olfactory fMRI could not be performed in 3 of the COVID-19 related OD and 2 of the post-infectious OD cases.

Parameters for DTI: TR = 10800 ms, TE = 116 ms, slice thickness/gap = 2/0 mm, number of slices = 70, FOV= 250 mm). Fat suppression was achieved with spectral presaturation using inversion recovery.

Parameters for fMRI: Functional images were gradient recalled echo-planar images with TR= 8000 ms; TE= 30 ms; FOV= 240×240 mm^2; slice thickness/gap = 2.5/0 mm and number of slices = 38. A total of 760 brain volume sequences were collected in 20 measurements during an interval of 3 minute and 6 seconds.

Olfactory Bulb MRI

Ultra-high resolution T2-SPACE (Sampling Perfection with Application optimized contrasts using different flip angle evolution) sagittal images (repetition time (TR)): 1000 ms, echo time (TE): 136 ms, flip angle: 110°, slice-thickness: 0.6 mm, slice oversampling: 0%, FOV: 200×200 mm, matrix: 320×320, phase oversampling: 30%, band width: 150 Hz/pixel, voxel size: 0.6×0.6×0.6 mm, time of acquisition: 6.08 minutes, echo-train duration: 440 ms)

Coronal T2 images covering anterior pole of the olfactory bulb to the primary olfactory region (TR: 6550 ms, TE: 99 ms, flip angle: 150°, slice-thickness: 1 mm, distance factor: 0, FOV: 100×100 mm², matrix: 269×384, phase oversampling: 56%, bandwidth: 289 Hz/pixel, voxel size: 0.3×0.3×1 mm, time of acquisition: 8.19 minutes, turbo factor: 17)

MRI Evaluation

Volumetric and morphological analysis were performed by a single radiologist.

Olfactory bulb volumes were calculated as summation of manually drawn sequential region of interests on consecutive coronal T2 slices with Syngo.Via Software (VB40, Siemens). Olfactory sulcus depth represented the distance between deepest point of the olfactory sulcus and a line tangent to the inferior borders of gyrus rectus and medial orbital gyrus. In order to calculate intra- and inter-observer variability, a second observer blind to previous measurements segmented olfactory bulb volumes twice in 23 cases. Intraclass coefficients of correlation between measurements of the 2 observers were 0.965 (95% CI 0.919− 0.985) for right OB, and 0.956 (95% CI 0.899− 0.981) for left OB. Intraclass coefficients of correlation between measurements of a single observer were 0.967 (95% CI 0.924− 0.986) for right OB, and 0.984 (95% CI 0.963− 0.993) for left OB.

Shape (morphology) of the olfactory bulb morphology was assessed on coronal T2-images. Olfactory bulbs normally have an oval or inverted-J shape (14,30). Multiple lobulations in the contour, rectangular shaped bulbs or atrophic bulbs were considered as abnormal in morphology.

The signal intensity of the olfactory bulbs was assessed on both coronal T2- and 3D-FLAIR images with contralateral gyrus rectus taken as the reference signal intensity. A single focus of abnormal signal intensity was not considered as abnormal due to artifact prone nature of the olfactory bulbs (31,32). Signal abnormalities were reviewed for location along the olfactory bulb (rostral, central, and caudal).

Olfactory nerve filiae were evaluated on the sagittal T2-space images. Normally olfactory nerve filiae show a fine architecture with uniform distribution of the filia at regular intervals. Focal thickening of the filiae with non-uniform distribution was considered as abnormal clumping.

DTI Data Analysis

Diffusion tensor images were processed with DSI studio (http://dsi-studio.labsolver.org). Image reconstruction was performed using generalized q-sampling imaging (GQI). Corrections for eddy currents distortions, motion artifacts and b-matrix reorientation were performed.

For network reconstruction, 90 grey matter regions of the cerebrum from the automated anatomical labeling (AAL) atlas was selected (33). Edge definition was performed with connectivity probability between each pair of nodes within the network. On connectogram maps, decreased connectivity was used to define a region with fiber tract number less than 50% or a QA value less than 50% compared to the contralateral region. Connectogram maps were categorized as: 0) normal connectivity, 1) decreased connectivity in rhinencephalon, 2) decreased connectivity in cingulate/insular cortex or thalamus, 3) decreased connectivity in other regions.

In addition, after manual seeding of orbitofrontal and enterorhinal cortex, the quantitative anisotropy (QA) and number of the fiber tracts of these regions and connecting fibers were automatically calculated by the software. Largest fiber deviation in one step was 10°, minimum fiber length was 5 mm, with a step size of 0.25 voxel.

fMRI Data Analysis

Preprocessing of the fMRI data was performed with Syngo. Via MR-NEURO 3D Software (VB40, Siemens) software. Correction of the echo-planar images (EPI) for slice-time differences and realignment to the first scan by rigid body transformation to correct for head motion were carried out. EPI and structural scans were normalized to the EPI standard template in the Montreal Neurological Institute space by linear and nonlinear transformations (maximum translation -00.86 mm, maximum rotation -00.26°) and final smoothing with a Gaussian kernel of 8-mm full width at half maximum. Fusion was completed in advanced perfusion mode by 50% blending after alignment. Images were displayed as hot metal colormap with a T-score cut-off value of 4.00. Positive activity was accepted as artifact free regions with a BOLD activity larger than 10 voxels after fusion. Positive activity was grouped as grade 1 for activity 10−100 voxels and grade 2 for activity larger than 100 voxels.

Extent of olfactory, trigeminosensory activity was categorized as the following: 1) orbitofrontal activity alone, 2) entorhinal activity alone, 3) both orbitofrontal and entorhinal (rhinencephalon) activity, 4) trigeminosensory activity, 5) activity outside the rhinencephalon or trigeminosensory system.

Statistical Analysis

All statistical analysis were carried out with NCSS (Number Cruncher Statistical System) Statistical Software (Utah, USA). Descriptive data were expressed as mean, standard deviation,

median and frequency. Group comparisons for continuous and categorical variables were performed with Student's t-test and Pearson's Chi squared-test, respectively. p value <0.05 was considered as statistically significant.

RESULTS

A total of 31 patients presenting with persistent COVID-19 related OD and 97 patients with post-infectious OD due to other viral pathogens were included. Mean age of the whole study population (n = 128) was 42.6±14.1 year (range 19−80 years) with a slight female predominance (n = 80, 62.5%). Patients with COVID-19 related OD were younger (32.5±10.8) than patients with post-infectious OD (45.9± 13.5) (p <0.001). There was no significant difference in female to male ratio in both groups (Table 1).

Patients with post-infectious OD presented later for olfactory evaluation than patients with COVID-19 related OD. Mean interval between onset of OD and evaluation was 1.5 months for COVID-19 related OD and 6 months for post-infectious OD (p <0.001). At the time of evaluation, all 128 patients were either hyposmic (n = 18, 14.1%) or anosmic (n = 110, 85.9%) based on TDI scores. All cases with COVID-19 related OD were anosmic (n=31, 100%), whereas 18 cases (18.6%) of post-infectious OD patients were hyposmic and remaining 69 cases (81.4%) were anosmic. Mean TDI score in COVID-19 related OD (9.31±2.89) was significantly lower than post-infectious OD (12.71±4.33) (p <0.001). Details on subsets of TDI scores can be found in (Table 1).

Olfactory Bulb MRI

Olfactory bulb volumes were significantly higher in COVID-19 related OD (right: 60.3±12.7 mm^3; left: 59.5±16.4 mm^3) than post-infectious OD (right: 48.6±15.4 mm^3; left: 48.9± 15.6 mm^3) (p <0.001 and p = 0.002, respectively) (Table 2).

There was no significant difference in olfactory sulcus depths between the two groups (Table 2).

Normal olfactory bulb morphology was preserved in 13 cases (41.9%) with COVID-19 related OD and 35 cases

TABLE 1. Demographic Data and TDI Scores for COVID-19 Related and Post-Infectious Olfactory Dysfunction

	COVID-19 (n = 31)	Post-Infectious (n = 97)	p
Age (mean±SD)	32.5±10.8	45.9±13.5	0.001
Sex (F/M)	21/10	59/38	0.489
TDI	9.31±2.89	12.71±4.33	0.001
T	2.10±1.31	4.07±1.52	0.001
D	3.52±1.26	4.28±1.37	0.003
I	3.74±1.03	4.58±1.68	0.009

T, odor detection thresholds; O, odor discrimination; I, odor identification.

TABLE 2. Comparison of Olfactory Bulb Volumes, Olfactory Sulcus Depths, Olfactory Bulb Morphology/Signal Intensity and Olfactory Filiae Architecture in COVID-19 Related and Post-Infectious Olfactory Dysfunction

	COVID-19 (n = 31)	Post-Infectious (n = 97)	p
R olfactory bulb volume (mm^3)	60.3±12.7	48.6±15.4	0.001
L olfactory bulb volume (mm^3)	59.5±16.4	48.9±15.6	0.002
R olfactory sulcus depth (mm)	6.80±2.0	6.50±2.1	0.469
L olfactory sulcus depth (mm)	6.30±2.1	6.20±2.0	0.886
Olfactory bulb morphology			0.558
Normal	13 (41.9)	35 (36.1)	
Deformed	18 (58.1)	62 (63.9)	
Olfactory bulb signal abnormality			
Central	8 (25.8)	23 (23.7)	0.813
Rostral	11 (35.5)	32 (33)	0.798
Caudal	0 (0)	3 (3.1)	1.000
Olfactory filia clumping			0.001
Absent	9 (29.0)	68 (70.1)	
Mild	20 (64.5)	29 (29.9)	
Marked	2 (6.5)	0	

(36.1%) with post-infectious OD. Deformed bulb morphology was seen in 18 cases (58.1%) with COVID-19 related OD and 62 cases (63.9%) with post-infectious OD; without significant difference between the groups (p = 0.558).

Olfactory bulb signals were normal in 15 patients (48.4%) with COVID-19 related OD and 52 patients (53.6%) with post-infectious OD. There was increased signal intensity in olfactory bulb in 16 patients (51.6%) with COVID-19 related OD. There was abnormally increased signal intensity in olfactory bulb in 45 patients (46.4%) with post-infectious OD, without significant difference between the two groups (Figs 1 and 2).

There was a significantly higher rate of olfactory nerve clumping in COVID-19 related OD than post-infectious OD (p <0.001). Normal olfactory nerve filia distribution were noted in 9 cases (29%) with COVID-19 related OD and 68 cases (70.1%) with post-infectious OD. Mild olfactory nerve clumping was noted in 29 cases (29.9%) with post-infectious OD, whereas there was mild olfactory nerve clumping in 20 cases (64.5%) and marked olfactory nerve clumping in 2 cases (6.5%) with COVID-19 related OD (Fig 3). (Table 2)
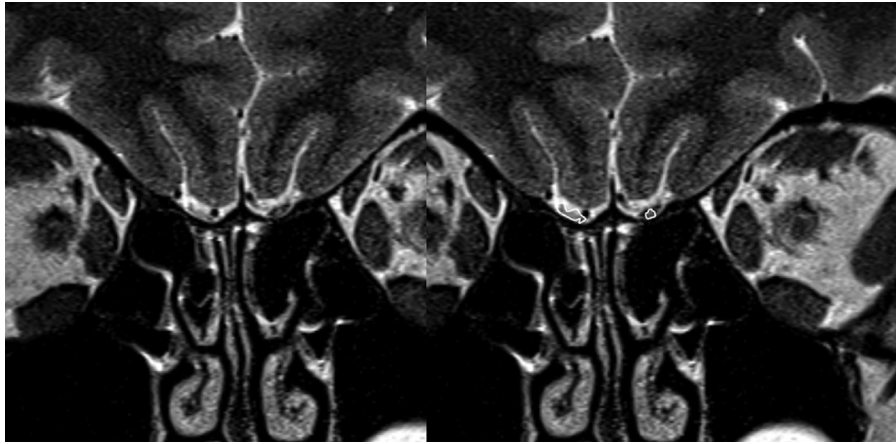
Olfactory Tract DTI

QA values at orbitofrontal, entorhinal region and orbitofrontal to entorhinal connections were significantly higher in COVID-19 related OD than post-infectious OD (p <0.001). Details of the QA values can be found in (Table 3) (Fig 4).

Connection fibers between orbitofrontal and entorhinal regions were affected similarly on the left and right side in
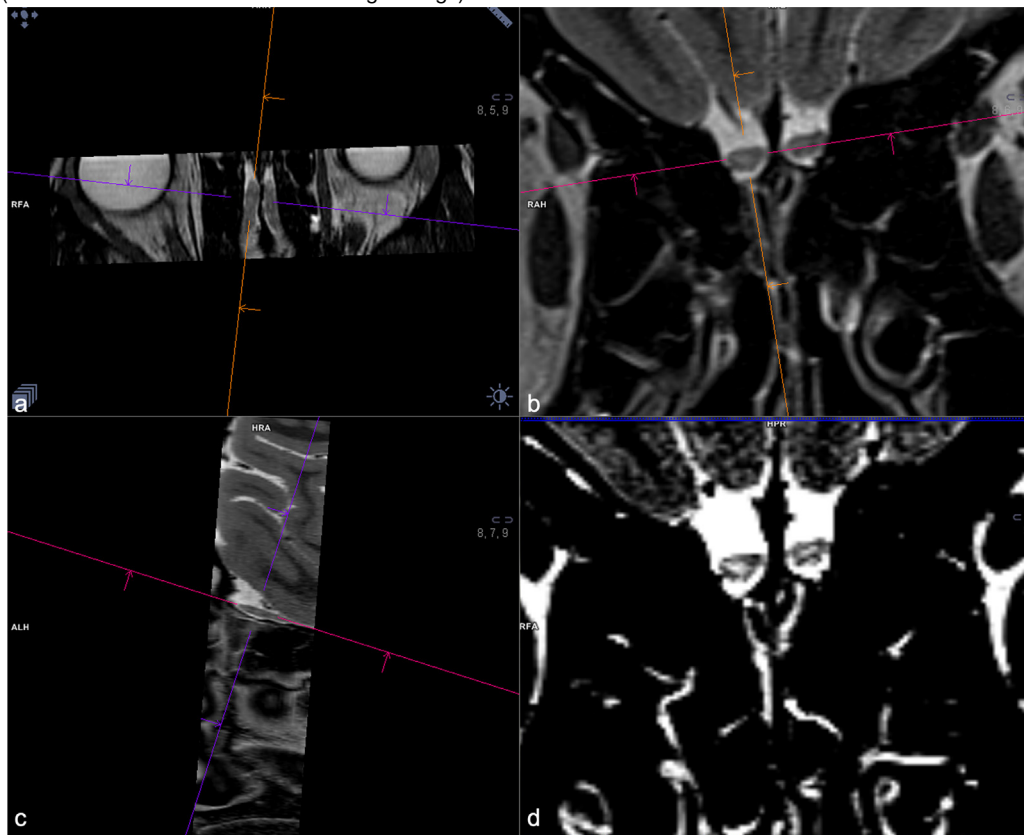
Figure 1. A 38-year-old female with functional anosmia for 2-months after COVID-19 infection. Coronal T2-WI show substantial volume loss of bilateral olfactory bulbs with internal areas of increased signal intensity localized to rostral olfactory tract on the right and caudal olfactory bulb on the left (delineated with free-hand ROI on the right image).


Figure 2. A 25-year-old female with functional anosmia for 6-weeks after COVID-19 infection COVID-19 related anosmia case. High resolution T2-SPACE images obtained on sagittal plane were viewed as multiplanar reformat images to assess olfactory bulb signal intensity (A-C). T2-W images show areas of increased signal intensity in bilateral olfactory bulbs, better seen on narrow window settings (D). (Color version of figure is available online.)

both COVID-19 related OD and post-infectious OD. Asymmetry in the connection fibers between left and right side were observed in 66.7% of COVID-19 related OD and 67% of post-infectious OD (p = 0.972). Visual scale of connectogram maps showed 42.3% dysconnectivity in post-infectious OD and 95.3% dysconnectivity in COVID-19 related OD (p <0.001) (Fig 5).

Olfactory fMRI

There was no significant difference in orbitofrontal activity alone and entorhinal activity alone between COVID-19 related OD and post-infectious OD (p = 0.963 and 0.228, respectively). Orbitofrontal activity was not observed in 32.1% of COVID-19 related OD and 29.5% of post-
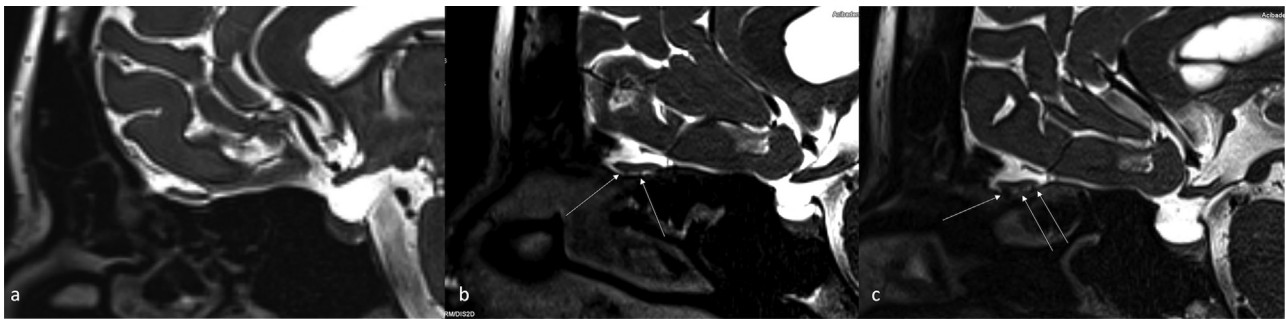
Figure 3. (A) Sagittal high resolution T2-SPACE image in a normal subject shows normal olfactory nerve filiae with no sign of clumping.

(B) A 32-year-old male with post-infectious olfactory dysfunction case. Sagittal T2-SPACE image shows clumping of the olfactory nerve filiae in the rostral portions (arrow). Normally, the olfactory nerve filiae are barely discernible, whereas in this case the filiae started to form bundles consistent with regenerative hypertrophy.

(C) A 28-year-old female with COVID-19 related anosmia. Sagittal SPACE image shows more extensive clumping and thickening of the olfactory nerve filiae (marked with multiple arrows) in the with significant effacement of CSF spaces caudal to the olfactory bulb.

TABLE 3. Comparison of Quantitative Anisotropy Values in COVID-19 Related and Post-Infectious Olfactory Dysfunction

	COVID-19 (n= 31)	Post- Infectious (n = 97)	p
R orbitofrontal gyrus, QA	331.5±64.9	259.5±101.3	0.001
L orbitofrontal gyrus, QA	338.2±71.3	266.5±102.5	0.001
R entorhinal gyrus, QA	377.9±89.2	270.1±100.3	0.001
L entorhinal gyrus, QA	382.9±100.6	270.3±102.1	0.001
R fibers from orbitofrontal to entorhinal area, QA	406.9±113.9	270.8±112.6	0.001
L fibers from orbitofrontal to entorhinal area, QA	431.2±114.5	280.5±116.3	0.001

infectious OD. Entorhinal activity was not observed in 60.7% of COVID-19 related OD and 45.3% of post–infectious OD.

Trigeminosensory activity was more robust in COVID-19 related OD cases (p = 0.005) (Table 4). Disorganized activity outside the rhinencephalon or trigeminosensory system was more prevalent in post-infectious OD (23.7%) compared to COVID-19 related OD (6.5%) (Fig 6).

DISCUSSION

In this study, we compared olfactory bulb MRI, olfactory tract DTI and olfactory fMRI findings in persistent COVID-19 anosmia and post-infectious OD due to other pathogens. Imaging was performed after a shorter duration in COVID-19 anosmia (mean 1.5-months) than post-infectious OD (mean 6-months). When compared to the post-infectious
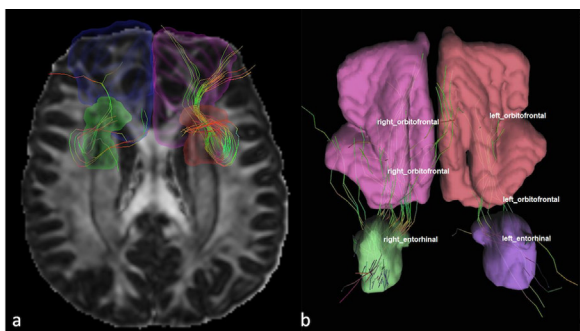
Tract Name and Area	Tracts between Right orbitofrontal and entorhinal field	Tracts between Left orbitofrontal and entorhinal field		
number of tracts	36	13		
tract length mean (mm)	77.75	79.2692		
qa mean	0.434591	0.407149		
Olfactory area	Right Orbitofrontal	Left Orbitofrontal	Right Entorhinal	Left Entorhinal
voxel counts	376.1	390.4	486.0	682.0
qa mean	0.29973	0.318064	0.363283	0.326646

Figure 4. A 37-year-old female with COVID-19 related anosmia. (A) Tractography images obtained with DSI studio by seeding the orbitofrontal regions and the entorhinal region (parahippocampal gyrus and amygdala) The tractography map shows decreased number of the fibers between right orbitofrontal and entorhinal regions compared to the contralateral tract. (B-C) Tractography images obtained with DSI studio by seeding the orbitofrontal regions and the entorhinal region (parahippocampal gyrus and amygdala) The tractography map shows decreased number of the fibers between left orbitofrontal and entorhinal regions compared to the contralateral tract. (C) Accompanying table showing number of tracts, mean tract length and QA values for the same case. (Color version of figure is available online.)
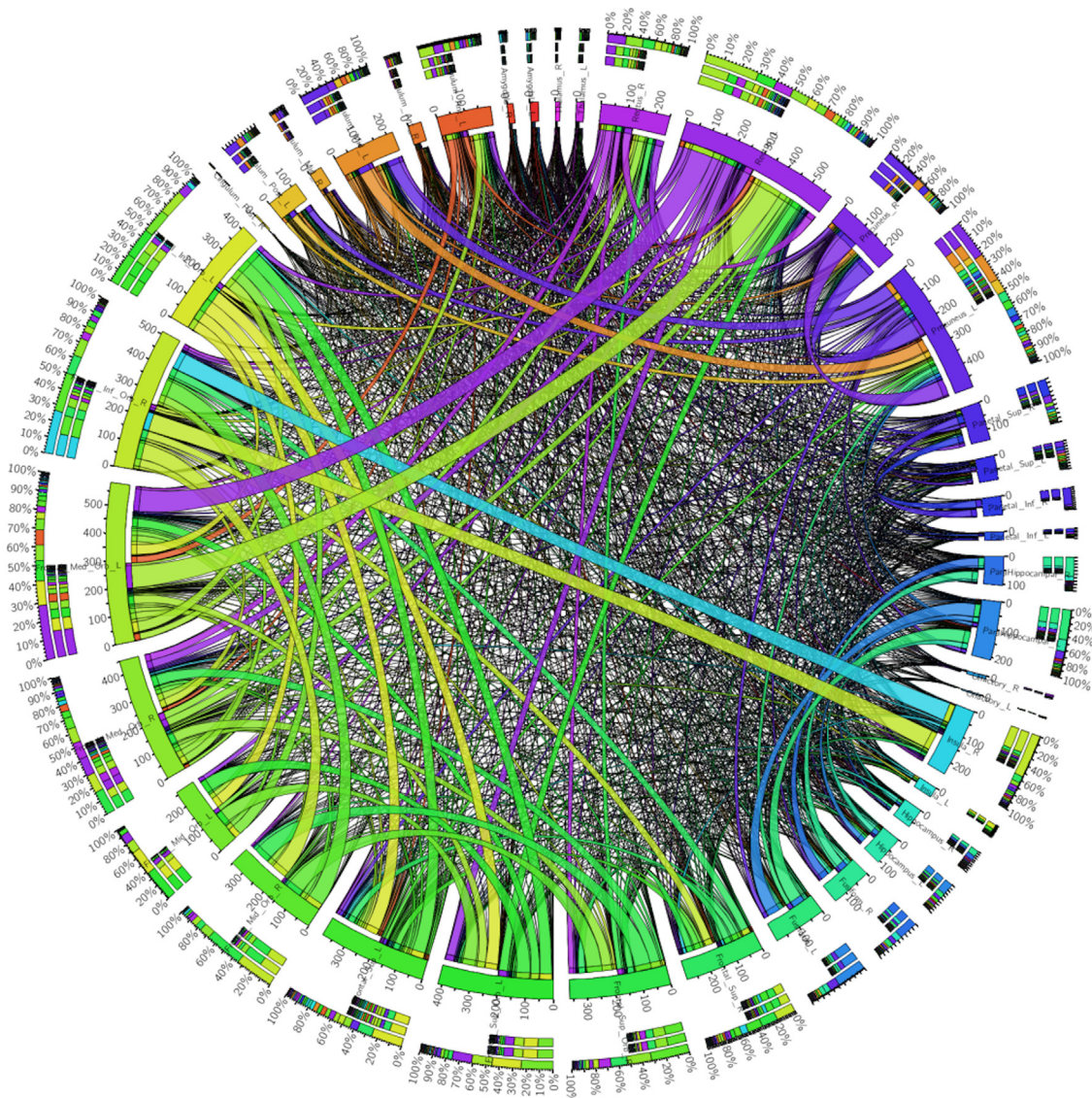
Figure 5. Connectogram map for the case presented in Figure 4. There is decreased connectivity between left insula and left olfactory cortex with possible compensatory increased connectivity in interfrontal, intrafrontal, intratemporal and tempofrontal regions. (Color version of figure is available online.)

OD, COVID-19 anosmia cases had better preservation of the olfactory bulb volumes, higher olfactory nerve clumping rates and better white matter integrity at secondary olfactory regions as demonstrated by higher QA values. There was no significant difference in olfactory bulb deformation or signal abnormality between the two groups. On fMRI, there was no significant difference in orbitofrontal activity alone and entorhinal activity alone between COVID-19 related OD and post-infectious OD, whereas trigeminosensory activity was more robust in COVID-19 related OD.

Olfactory Bulb Volumes

Olfactory bulb functions as the first relay station in the olfactory pathway (15). Olfactory bulb maintains its high plasticity throughout the life through its continuing synaptogenesis

(13,34). A distinguishing feature of olfactory system is decreased olfactory bulb volume with olfactory deprivation supported by positive correlation between olfactory function and olfactory bulb volume (35). Studies have demonstrated decreased olfactory bulb volume with olfactory loss in post-traumatic OD, post-infectious OD and neurodegenerative diseases. In our series, though both COVID-19 anosmia and post-infectious OD cases had mildly decreased olfactory bulb volumes when 58 mm^3 cut-off value for patients <45 years of age as defined by Buschhüter et al. is used olfactory volume loss was more pronounced in post-infectious OD than COVID-19 anosmia (35). This is unlikely related to degree of olfactory loss, as TDI scores in COVID-19 anosmia were lower in our cohort. A likely explanation for lower olfactory bulb volume in post-infectious OD than COVID-19 related OD is duration of olfactory deprivation as time to imaging

TABLE 4. Comparison of Activation Of Different Regions after Olfactory fMRI with n-Butanol in COVID-19 Related and Post-Infectious Olfactory Dysfunction

		COVID-19		Post- Infectious		p
		n	%	n	%	
Orbitofrontal activity	No activity	9	32.1%	28	29.5%	0.963
	1*	14	50.0%	49	51.6%	
	2#	5	17.9%	18	18.9%	
Entorhinal activity	No activity	17	60.7%	43	45.3%	0.228
	1*	10	35.7%	40	42.1%	
	2#	1	3.6%	12	12.6%	
Trigeminosensory activity	No activity	18	64.3%	85	89.5%	0.005
	1*	6	21.4%	5	5.3%	
	2#	4	14.3%	5	5.3%	
Outside the rhinencephalon or trigeminosensory system	Activity	2	6.5%	23	23.7%	0.128

* Grade 1: activity 10−100 voxel size,
# grade 2: activity larger than 100 voxels.
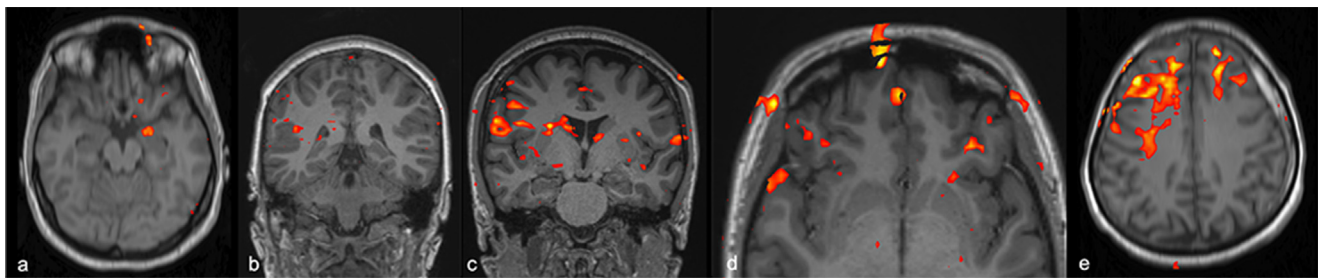
Figure 6.   Olfactory fMRI with n-butanol. Fused 3D T1 and bold images shows activity in leftorbitofrontal and entorhinal region in a post-infectious OD case (A); right trigeminosensorial region in a COVID-19 related anosmia case (B); bilateral trigeminosensorial regions more prominent on the right side, without discernible activity in the bilateral entorhinal regions in a COVID-19 related anosmia case (C); bilateral orbitofrontal region in a COVID-19 related anosmia case (D); disorganized, diffuse activity outside the olfactory region in a post-infectious OD case (E). (Color version of figure is available online.)

since OD onset was longer in post–infectious OD in our series. This finding is in line with a post–infectious OD MRI study by Rombaux et al. where there was a moderate degree of negative correlation between olfactory bulb volumes and duration of olfactory loss (36).

Olfactory Bulb Morphology and Signal Intensity

MRI can also be interpreted for olfactory bulb shape where loss of normal oval or inverted J shape is suggestive of damage (37). In addition, abnormally increased signal intensities in the olfactory bulb are indicative of degeneration (14). Studies on olfactory bulb imaging in COVID-19 OD are limited in terms of imaging protocols and timing through the course of the OD. Majority of the studies report findings based on conventional cranial images instead of dedicated thin-cut, high resolution sequences. Some of the studies lack objective olfactory testing, and timing of imaging varied among the studies (1,21-24,38,39). Available olfactory bulb imaging literature on COVID-19 anosmia is variable with reports of grossly normal olfactory bulb volumes without signal abnormality or olfactory bulb signal abnormality in the form of increased signal or abnormal enhancement.(1,40). Some of

the reports showed return of olfactory bulb intensity back to normal in follow-up imaging after olfactory function recovery (24,39). In our series, there was increased signal intensity in olfactory bulb in 16 patients (51.6%) with COVID-19 related OD. This rate was not significantly different compared to the 46.4% of abnormal bulb signal intensity we noted in post-infectious OD.

One potential caveat in assessment of olfactory bulb hyperintensity is signal intensity can vary according to the field strength applied and acquisition parameters especially on 3D-FLAIR images. Healthy subjects may have olfactory bulbs hyperintensities on 3D-FLAIR images (41). Despite this potential pitfall, recent literature using normalized olfactory bulb signal intensity reported higher olfactory bulb T2 FLAIR signal intensity between the patients with COVID-19 and the controls with anosmia (42).

In our series, we observed a significantly higher rate of olfactory nerve clumping in COVID-19 related OD than post-infectious OD. Clumping of the olfactory nerve filia are suggestive of inflammatory changes and regenerative attempt by the olfactory nerve (14). The higher rate of clumping in COVID-19 anosmia might be related to a more robust regeneration attempt within the subacute phase of OD as

compared to post-infectious OD. The sustentacular cells have a good regenerative capacity which improves recovery of olfaction (43,44).

Olfactory Tract DTI

DTI provides data on directionality of water diffusion and information on microstructural brain damage can be derived (15). The most commonly used DTI parameter is fractional anisotropy where higher values reflect greater directionality of diffusion, thus preserved microstructure (45). Previous DTI studies have shown reduced fractional anisotropy in olfactory impairment due to trauma, aging and neurodegenerative diseases (46). Additionally, there is improvement of white matter integrity in with chronic rhinosinusitis after sinus surgery, which may be a sign of cerebral plasticity (16). In our study, QA values in olfactory regions and tracts were higher in COVID-19 anosmia compared to post-infectious OD indicating better preserved integrity of the white matter tracts.

fMRI

Olfactory fMRI since its introduction by Yousem et al. has been mainly used in OD seen in neurodegenerative diseases, schizophrenia, congenital anosmia/hyposmia and more recently in post-traumatic OD (19,47-49). The olfactory neural network consists of the first-order projections to piriform cortex and amygdala and secondary projections to the orbitofrontal cortex, thalamus, and insula (50).

In our study, we observed no significant difference in orbitofrontal activity alone and entorhinal activity alone between COVID-19 related OD and post-infectious OD. A PET-MR study on 12 cases with COVID-19 related olfactory loss reported regional glucose metabolism abnormalities in olfactory and high-order brain networks which changed with intensity and duration of the anosmia (51).

In our series, we observed a more robust trigeminosensory activity in COVID-19 related OD compared to post-infectious OD. The olfactory and trigeminal systems have a complex relationship in detection of odor. Most odorants also result in stimulation of the trigeminal system. Prior studies on acquired anosmia showed that olfactory loss produces central nervous system changes that lead to a reduced responsiveness to trigeminal stimulation (52). The higher trigeminosensory activity observed among COVID-19 related OD in our series reflect the higher degree of central olfactory system damage observed in post-infectious OD as demonstrated by greater olfactory bulb volume loss and less well-preserved integrity of the white matter tracts in post-infectious OD compared to COVID-19 related OD.

Pathogenesis

Pathogenesis of COVID-19 related olfactory dysfunction is incompletely understood. Potential mechanisms are damage to the olfactory epithelium secondary to inflammation, or direct damage to olfactory epithelium or bulb (53). Olfactory epithelium damage seems more plausible as angiotensin converting enzyme 2 (ACE2) receptors, the target molecules for SARS-CoV-2, are expressed by non-neuronal supporting cells of the olfactory epithelium, but not directly by the olfactory neurons (53).

In post-infectious olfactory loss; early phase is characterized by a conductive or obstructive olfactory loss related to mucosal edema. Olfactory function typically recovers with amelioration of the cold symptoms. However, in a small percentage of patients, there is persistent olfactory loss despite absence of nasal congestion or obstruction. In such cases, the olfactory loss reflects sensorineural pathway damage related to the viral insult (54). Significantly reduced olfactory receptor cells and nerve bundles have been reported in the olfactory epithelium in post-infectious OD cases support this hypothesis (55,56).

Limitations of the current study include the different interval between onset of olfactory loss and imaging evaluation in COVID-19 and post-infectious OD. This created a variable that might have accounted for the different imaging findings we observed between the 2 groups as described above. There is also a selection bias, as only patients with persistent COVID-19 OD longer than 1-month in duration were evaluated. This inherently excluded patients with shorter and milder olfactory loss, limiting generalizability of the findings to worst olfactory loss case scenario. Also, our imaging findings may reflect the subacute and chronic state of changes, rather than the acute changes. There are different block designs available in the literature which migh affect the pattern of activity. A study by Poellinger et al. showed that short-duration stimulus (9 seconds) consistently activated the primary olfactory cortex, whereas long stimulus (60 seconds) resulted in short, phasic increase in the signal, followed by a prolonged decrease below baseline in the primary olfactory cortex and hippocampus (57). Orbitofrontal cortex activity was present during the duration of odorant presentation. The long stimulus design parameter of our study might have affected pattern of activation and limits comparison to other studies.

CONCLUSION

Our study with incorporation of different anatomical and functional imaging modalities indicates that olfactory bulb damage may play a role in COVID-19 anosmia seen as abnormal shape and signal intensity of the olfactory bulbs. Though there is decreased olfactory bulb volume, this is not as pronounced as in other post-infectious OD, likely reflecting earlier imaging done in COVID-19 cases with limited duration of olfactory deprivation to result in olfactory bulb volume loss. We observed a higher rate of olfactory nerve clumping in COVID-19 anosmia compared to post-infectious OD, indicating a higher degree of active regeneration attempt. The white matter tract integrity of olfactory regions was better preserved in COVID-19 anosmia compared to

post–infectious OD, which also might be related to shorter imaging duration since onset of olfactory loss. There was no significant difference in orbitofrontal activity alone and entorhinal activity alone between COVID-19 related OD and post–infectious OD, whereas trigeminosensory activity was more robust in COVID-19 related OD. The higher trigeminosensory activity observed among COVID-19 related OD in our series may reflect better preserved central olfactory system in COVID-19 related OD compared to COVID-19 related OD.

REFERENCES

1. Galougahi MK, Ghorbani J, Bakhshayeshkaram M, Naeini AS, Haseli S. Olfactory bulb magnetic resonance imaging in SARS-CoV-2-induced anosmia: the first report. Acad Radiol 2020; 27:892–893.
2. Cooper KW, Brann DH, Farruggia MC, et al. COVID-19 and the chemical senses: supporting players take center stage. Neuron 2020; 107:219–233.
3. Altundag A, Saatci O, Sanli DET, et al. The temporal course of COVID-19 anosmia and relation to other clinical symptoms. Eur Arch Otorhinolaryngol 2021; 278:1891–1897.
4. Lechien JR, Journe F, Hans S, et al. Severity of anosmia as an early symptom of COVID-19 infection may predict lasting loss of smell. Front Med (Lausanne) 2020; 7:582802.
5. Moein ST, Hashemian SM, Tabarsi P, Doty RL. Prevalence and reversibility of smell dysfunction measured psychophysically in a cohort of COVID-19 patients. Int Forum Allergy Rhinol 2020; 10:1127–1135.
6. Vaira LA, Hopkins C, Petrocelli M, et al. Smell and taste recovery in coronavirus disease 2019 patients: a 60-day objective and prospective study. J Laryngol Otol 2020; 134:703–709.
7. Cavazzana A, Larsson M, Münch M, Hähner A, Hummel T. Postinfectious olfactory loss: a retrospective study on 791 patients. Laryngoscope 2018; 128:10–15.
8. Nordin S, Brämerson A. Complaints of olfactory disorders: epidemiology, assessment and clinical implications. Curr Opin Allergy Clin Immunol 2008; 8:10–15.
9. Seiden AM, Duncan HJ. The diagnosis of a conductive olfactory loss. Laryngoscope 2001; 111:9–14.
10. Temmel AF, Quint C, Schickinger-Fischer B, Klimek L, Stoller E, Hummel T. Characteristics of olfactory disorders in relation to major causes of olfactory loss. Arch Otolaryngol Head Neck Surg 2002; 128:635–641.
11. Moonis G, Mitchell R, Szeto B, Lalwani AK. Radiologic assessment of the sinonasal tract, nasopharynx and mastoid cavity in patients with sars-cov-2 infection presenting with acute neurological symptoms. Ann Otol Rhinol Laryngol 2021; 130(11):1228–1235. doi:10.1177/0003489421995070:3489421995070.
12. Jalessi M, Barati M, Rohani M, et al. Frequency and outcome of olfactory impairment and sinonasal involvement in hospitalized patients with COVID-19. Neurol Sci 2020; 41:2331–2338.
13. Rombaux P, Duprez T, Hummel T. Olfactory bulb volume in the clinical assessment of olfactory dysfunction. Rhinology 2021; 47:3–9. 200.
14. Yildirim D, Altundag A, Tekcan Sanli DE, et al. A new perspective on imaging of olfactory dysfunction: does size matter? Eur J Radiol 2020; 132:109290.
15. Bonanno L, Marino S, De Salvo S, et al. Role of diffusion tensor imaging in the diagnosis and management of post-traumatic anosmia. Brain Inj 2017; 31:1964–1968.
16. Güllmar D, Seeliger T, Gudziol H, et al. Improvement of olfactory function after sinus surgery correlates with white matter properties measured by diffusion tensor imaging. Neuroscience 2017; 360:190–196.
17. Nigro P, Chiappiniello A, Simoni S, et al. Changes of olfactory tract in Parkinson's disease: a DTI tractography study. Neuroradiology 2021; 63:235–242.
18. Skorpil M, Rolheiser T, Robertson H, Sundin A, Svenningsson P. Diffusion tensor fiber tractography of the olfactory tract. Magn Reson Imaging 2011; 29:289–292.
19. Moon WJ, Park M, Hwang M, Kim JK. Functional MRI as an objective measure of olfaction deficit in patients with traumatic anosmia. AJNR Am J Neuroradiol 2018; 39:2320–2325.
20. Wang J, Eslinger PJ, Doty RL, et al. Olfactory deficit detected by fMRI in early Alzheimer's disease. Brain Res 2010; 1357:184–194.
21. Strauss SB, Lantos JE, Heier LA, Shatzkes DR, Phillips CD. Olfactory bulb signal abnormality in patients with COVID-19 who present with neurologic symptoms. AJNR Am J Neuroradiol 2020; 41:1882–1887.
22. Corrêa DG, Hygino da Cruz LC, Lopes FCR, et al. Magnetic resonance imaging features of COVID-19-related cranial nerve lesions. J Neurovirol 2021; 27:171–177.
23. Eliezer M, Hautefort C. MRI Evaluation of the olfactory clefts in patients with SARS-CoV-2 infection revealed an unexpected mechanism for olfactory function loss. Acad Radiol 2020; 27:1191.
24. Laurendon T, Radulesco T, Mugnier J, et al. Bilateral transient olfactory bulb edema during COVID-19−related anosmia. Neurology 2020; 95:224–225.
25. Kandemirli SG, Altundag A, Yildirim D, Tekcan Sanli DE, Saatci O. Olfactory bulb mri and paranasal sinus ct findings in persistent COVID-19 anosmia. Acad Radiol 2021; 28:28–35.
26. Kobal G, Hummel T, Sekinger B, Barz S, Roscher S, Wolf S. Sniffin' sticks": screening of olfactory performance. Rhinology 1996; 34:222–226.
27. Hummel T, Kobal G, Gudziol H, Mackay-Sim A. Normative data for the "Sniffin' Sticks" including tests of odor identification, odor discrimination, and olfactory thresholds: an upgrade based on a group of more than 3,000 subjects. Eur Arch Otorhinolaryngol 2007; 264:237–243.
28. Jacquot L, Monnin J, Brand G. Influence of nasal trigeminal stimuli on olfactory sensitivity. C R Biol 2004; 327:305–311.
29. Boyle JA, Frasnelli J, Gerber J, Heinke M, Hummel T. Cross-modal integration of intranasal stimuli: a functional magnetic resonance imaging study. Neuroscience 2007; 149:223–231.
30. Schneider JF, Floemer F. Maturation of the olfactory bulbs: mr imaging findings. Am J Neuroradiol 2009; 30:1149–1152.
31. Leboucq N, Menjot de Champfleur N, Menjot de Champfleur S, Bonafé A. The olfactory system. Diagn Interv Imaging 2013; 94:985–991.
32. Tsutsumi S, Ono H, Yasumoto Y. Visualization of the olfactory nerve using constructive interference in steady state magnetic resonance imaging. Surg Radiol Anat 2017; 39:315–321.
33. Tzourio-Mazoyer N, Landeau B, Papathanassiou D, et al. Automated anatomical labeling of activations in SPM using a macroscopic anatomical parcellation of the MNI MRI single-subject brain. Neuroimage 2002; 15:273–289.
34. Lledo PM, Gheusi G. Olfactory processing in a changing brain. Neuroreport 2003; 14:1655–1663.
35. Buschhüter D, Smitka M, Puschmann S, et al. Correlation between olfactory bulb volume and olfactory function. Neuroimage 2008; 42:498–502.
36. Rombaux P, Mouraux A, Bertrand B, Nicolas G, Duprez T, Hummel T. Olfactory function and olfactory bulb volume in patients with postinfectious olfactory loss. Laryngoscope 2006; 116:436–439.
37. Chung MS, Choi WR, Jeong HY, Lee JH, Kim JH. MR imaging-based evaluations of olfactory bulb atrophy in patients with olfactory dysfunction. AJNR Am J Neuroradiol 2018; 39:532–537.
38. Aragão M, Leal MC, Cartaxo Filho OQ, Fonseca TM, Valença MM. Anosmia in COVID-19 associated with injury to the olfactory bulbs evident on MRI. AJNR Am J Neuroradiol 2020; 41:1703–1706.
39. Politi LS, Salsano E, Grimaldi M. Magnetic resonance imaging alteration of the brain in a patient with coronavirus disease 2019 (COVID-19) and anosmia. JAMA Neurology 2020; 77:1028–1029.
40. Hatipoglu N, Yazici ZM, Palabiyik F, Gulustan F, Sayin I. Olfactory bulb magnetic resonance imaging in SARS-CoV-2-induced anosmia in pediatric cases. Int J Pediatr Otorhinolaryngol 2020; 139:110469.
41. Shor N, Chougar L, Pyatigorskaya N. MR imaging of the olfactory bulbs in patients with COVID-19 and anosmia: how to avoid misinterpretation. Am J Neuroradiol 2021; 42(3). doi:10.3174/ajnr.A6921.
42. Strauss SB, Lantos JE, Heier LA, Shatzkes DR, Phillips CD. Olfactory bulb signal abnormality in patients with COVID-19 who present with neurologic symptoms. Am J Neuroradiol 2020; 41:1882.
43. Brann DH, Tsukahara T, Weinreb C, et al. Non-neuronal expression of SARS-CoV-2 entry genes in the olfactory system suggests mechanisms underlying COVID-19-associated anosmia. Sci Adv 2020; 6(31).
44. Otte MS, Bork ML, Zimmermann PH, Klussmann JP, Luers JC. Persisting olfactory dysfunction improves in patients 6 months after COVID-19 disease. Acta Otolaryngol 2021. doi:10.1080/00016489.2021.1905178:1-4.
45. Han P, Zang Y, Akshita J, Hummel T. Magnetic resonance imaging of human olfactory dysfunction. Brain Topogr 2019; 32:987–997.

46. Chen B, Akshita J, Han P, Thaploo D, Kitzler HH, Hummel T. Aberrancies of brain network structures in patients with anosmia. Brain Topogr 2020; 33:403–411.

47. Yousem DM, Williams SC, Howard RO, et al. Functional MR imaging during odor stimulation: preliminary data. Radiology 1997; 204:833–838.

48. Schneider F, Habel U, Reske M, Toni I, Falkai P, Shah NJ. Neural substrates of olfactory processing in schizophrenia patients and their healthy relatives. Psychiatry Res Neuroimaging 2007; 155:103–112.

49. Wang J, Eslinger PJ, Doty RL, et al. Olfactory deficit detected by fMRI in early Alzheimer's disease. Brain Res 2010; 1357:184–194.

50. Yousem DM, Oguz KK, Li C. Imaging of the olfactory system. Semin Ultrasound CT MR 2001; 22:456–472.

51. Niesen M, Trotta N, Noel A, et al. Structural and metabolic brain abnormalities in COVID-19 patients with sudden loss of smell. Eur J Nucl Med Mol Imaging 2021; 48:1890–1901.

52. Frasnelli J, Schuster B, Hummel T. Interactions between olfaction and the trigeminal system: what can be learned from olfactory loss. Cereb Cortex 2007; 17:2268–2275.

53. Han AY, Mukdad L, Long JL, Lopez IA. Anosmia in COVID-19: mechanisms and significance. Chemical Senses 2020; 45:423–428.

54. Seiden AM. Postviral olfactory loss. Otolaryngol Clin North Am 2004; 37:1159–1166.

55. Yao L, Yi X, Pinto JM, et al. Olfactory cortex and Olfactory bulb volume alterations in patients with post-infectious Olfactory loss. Brain Imaging Behav 2018; 12:1355–1362.

56. Jafek BW, Murrow B, Michaels R, Restrepo D, Linschoten M. Biopsies of human olfactory epithelium. Chemical Senses 2002; 27:623–628.

57. Poellinger A, Thomas R, Lio P, et al. Activation and habituation in olfaction—an fMRI study. Neuroimage 2001; 13:547–560.